AUT Journal of Mechanical Engineering

AUT J. Mech. Eng., 3(1) (2019) 107-112
DOI: 10.22060/ajme.2018.14283.5719

An Experimental Study on Submerged Flame in a Two-Layer Porous Burner

S. A. Hashemi*, M. R. Faridzadeh

Department of Mechanical Engineering, University of Kashan, Kashan, Iran.

ABSTRACT: Combustion in porous media is an effective method to minimize dissipations and save energy. Therefore, Study on the porous burners has been the focus of many researches in the past decade, due to the favorable features of these burners. The conditions for the formation of a steady-state submerged flame in a ceramic (Silicon Carbide) porous medium were investigated at four firing rates. The results were obtained on a ceramic foam with a cross section area of 63.6 cm2 and pore density of either 10 or 30 ppi. The reactants were air and natural gas with various equivalence ratios. In this experimental study, eight thermocouples were mounted on the burner walls along its axis in order to track the flame position, and the results were presented as temperature profiles of the porous wall. It was observed that the formation of submerged flame depends on firing rate and equivalence ratio. The stability limit of submerged flame (the range between surface flame and flash back limits) is reduced by increasing the firing rate. Results show when the mixture velocity low, the stability limit extends. Finally, the ranges of equivalence ratio and mixture velocity for the formation of submerged flame are presented at various firing rates.

Review History:

Received:
Revised:
Accepted:
Available Online:

Keywords:

Experimental study
Flame formation
Porous burner
Premixed methane-air combustion

1- Introduction

Applying porous media in burners is known as an effective technique to reduce fuel consumption and emissions. High radiation efficiency, high flame speed and efficiency, high power density, reduced burner volume, improved flammability limit, uniform heat distribution, reduced noise and emission are among the advantages of porous burners over the common ones.

The earliest studies on combustion in porous media were carried out to create a flame with excess enthalpy. Drawing on the thermodynamic properties, Weinberg [1] showed that maximum flame temperature can be achieved through using a reactant preheating system that relies on combustion products. In their study, Weinberg found that the excess-enthalpy-flame can lead to steady combustion of low energy fuels. Younis and Viskanta [2] studied the effect of pore diameter on the volumetric heat transfer coefficient in alumina foam. They proposed multiple equations to calculate the volumetric Nusselt number in porous media. Khanna et al. [3] addressed the premixed combustion of methane-air mixture in a two-stage porous burner. They found the flame to be stable in the speed range of 15 to 48 cm/s.

Randrianalisoa et al. [4] attempted to design a porous burner with minimum emission and maximum thermal power. They first carried out a series of experiments in order to select the best material. Two experiments were considered for each material; one at the higher operating condition zones of the burner and the other at the lower zones. As for the minimum emission, metallic foams such as FeCrAlY offered the best performance under both operating conditions. No overall conclusion was made in this study on what is the best material. Bakri et al. [5] experimentally investigated combustion in a porous medium under various input pressure and temperature conditions. They realized that the flame moves downstream of the burner by increasing the pressure and preheating the input cone.

Keramiotis et al. [6] comprehensively investigated the thermal efficiency, emission, and the operating range of the porous burner. Their combustion chamber was a rectangular two-layer porous burner, the first layer of which was alumina and the second layer was a Silicon Carbide (SiC) foam. Methane and propane were used as fuel. The stability range was obtained based on various thermal loads and equivalence ratios. Gas temperature was measured by a thermocouple while the temperature of the solid was measured by an infra-red camera and emissions were recorded by a gas analyzer system. The results showed a uniform temperature distribution, low production of CO and NO_x and a fairly good stability range. Shi et al. [7] experimentally and numerically investigated flame stability in a porous medium. They studied the separation and deviation of the flame resulting from combustion of a lean mixture of methane and air. They observed that the separation and deviation of the flame in a 3 mm thick quartz tube filled with alumina shots at equivalence ratios ranging from 0.435 to 0.490. They investigated the impact of equivalence ratio on separation and deviation. It was found that the equivalence ratio significantly affects the

*Corresponding author's email: Hashemi@kashanu.ac.ir

separation and deviation of the flame. Moreover, the results suggested that separation takes place when deviation reaches 54˚-60˚.

Wang et al. [8] experimentally investigated the axial temperature variations of premixed methane-air combustion in a porous burner. In this study, details are given on the variations of gas temperature during the process of turning the burner on and off. The porous burner under study is composed of a cylinder filled with alumina, where the effects of gas flow, the diameter of alumina particles and the equivalence ratio on the variation of the axial temperature of the burner were examined. The results indicated that superadiabatic combustion (attaining a temperature higher than that of the adiabatic flame temperature) can take place and the critical equivalence ratio for the superadiabatic combustion is larger for smaller particles and higher air input. Gao et al. [9] addressed the premixed methane-air combustion in a two-stage porous burner. They compared three types of alumina porous media, namely sponge, granular, and honeycomb structures. The preheating zone was filled with granular alumina and the combustion zone (flame zone) was filled with one of the mentioned structures. One result of the study was the stability limit of the flame in these burners. The sponge structure was associated with the highest stability limit.

Stelzner et al. [10] investigated the flame structure in the lean methane-air combustion in a porous medium using advanced laboratory equipment. They employed the Laser-Induced Fluorescence (LIF) technique to determine the concentration of hydroxyl radicals (OH). The porous burner was a two-stage 135*185 mm rectangular burner with alumina preheating section and SiC combustion zone. The effect of thermal load on flame front in a porous medium was studied in the range of 200-800 kW/m^2. It was concluded that in same thermal loads, and within the steady operation limit of the burner, the location of maximum hydroxyl concentration is almost independent of the ratio of excess air. Moreover, it was found that the length of the flame zone increases with the ratio of excess air. Shakiba et al. [11] experimentally investigated the effect of foam structure and material on the operation of a porous ceramic burner. Alumina and silicon carbide foams with porosities of 74 to 80% and pore density of 10 to 30 ppi were tested in this study. The maximum combustion temperature was not achieved through the stoichiometric ratio, but at 20% excess air. They found that thermal efficiency in foams with larger pores (smaller pore density) considerably increases with excess air. In foams with smaller pores, however, the variation is less.

Liu et al. [12] numerically investigated the effect of thermal conductivity of the burner wall on flame stability and the efficiency of methane-air combustion in a porous media containing fibers. They showed both lower and upper bounds for stability in the burner to increase with the conductivity of the burner walls. Their quantitative investigation showed that two main factors are involved in this behavior: 1) increase in thermal improvement with the conductivity of the burner wall, which can lead to a higher burning rate of the gas mix, and 2) dead zone (quenched zone) near the walls grows larger as the conductivity of the burner wall increases and the wall temperature decreases. Furthermore, it should be noted that the growth of the dead zone reduces combustion efficiency. Therefore, in a small channel filled with porous medium containing fibers, a solid wall with a relatively small conductivity is a good choice for the burner. Emami et al. [13] experimentally studied a two-layer porous burner in which the first layer was SiC and the second one was composed of aluminum silicate (Al_2SiO_5) balls. They investigated the effect of ball diameter in the downstream, the equivalence ratio, and firing rate on flame temperature, stability limit of the flame, flashback, and emissions. The results indicated that the flame was stabilized in the equivalence ratio range of 0.35-0.45 inside the porous medium. Decreasing the equivalence ratio, the flame moves downstream. Moreover, increasing the ball diameter downstream of the burner, the maximum flame temperature and the flame surface temperature are reduced. Increasing the equivalence ratio, the flashback time is reduced. Additionally, flashback time is reduced as pore density is increased downstream of the burner.

Ghorashi et al. [14] experimentally measured the pollutant emissions in a novel combined porous-free flame burner and compared it with a porous burner. They showed that CO concentration in the porous-free flame burner is lower than that of the porous burner and NO_x concentration changes only with varying the equivalence ratio and other parameters have no significant effect on NO_x emission. Hashemi and Hashemi [15] numerically analyzed the flame stabilization of a premixed methane-air combustion within a two-layer porous burner. Their results showed that the stability limit and flame temperature within a porous burner can be controlled by the equivalence ratio of the incoming mixture. In another work, they numerically studied a premixed methane–air combustion process within a combined porous-free flame burner. Comparison of the combined porous-free flame burner with porous burner showed that the flame stability limits of the combined burner were higher than those of porous burner also investigation of the effect of pore density on the flame stabilization showed that the lower pore densities were desirable in order to improve the flame stability limits [16].

In the present study, the conditions in which a submerged flame can be stabilized in a two-layer burner is investigated. The effect of the equivalence ratio, firing rate and the mixture velocity on the flame stability will be experimentally investigated. Finally the diagram of the stability range is plotted and compared with the other works [17]. Obtaining the stability range (buried flame stability), as well as obtaining the conditions in which the flame is stable within the porous medium, and the process of stabilizing the flame inside the ceramic porous medium (combinations of 10 and 30 ppi) can be mentioned as novelties of the presented paper.

2- Apparatus

A schematic view of the designed apparatus is shown in Fig. 1. The porous media used in this study are SiC cylindrical ceramic foams with a diameter of 90 mm and a height of 21 mm and pore density of either10 or 30 ppi. The first layer is 30 ppi and the second layer is 10 ppi. The properties of this type of ceramic are presented in Table 1. In order to maintain the ceramic piece in a vertical direction, an alumina retainer with an inner diameter of 88 mm and a wall thickness of 46 mm were used. As shown in Fig. 2, there are 8 mm holes on the lateral walls of the ceramic piece located in a center-to-center vertical distance of 5 mm. Eight thermocouples are used in the experiment, numbered from 1 to 8 along the burner in the flow direction. Thermocouple 1 was installed at the beginning of the first layer and the last thermocouple was

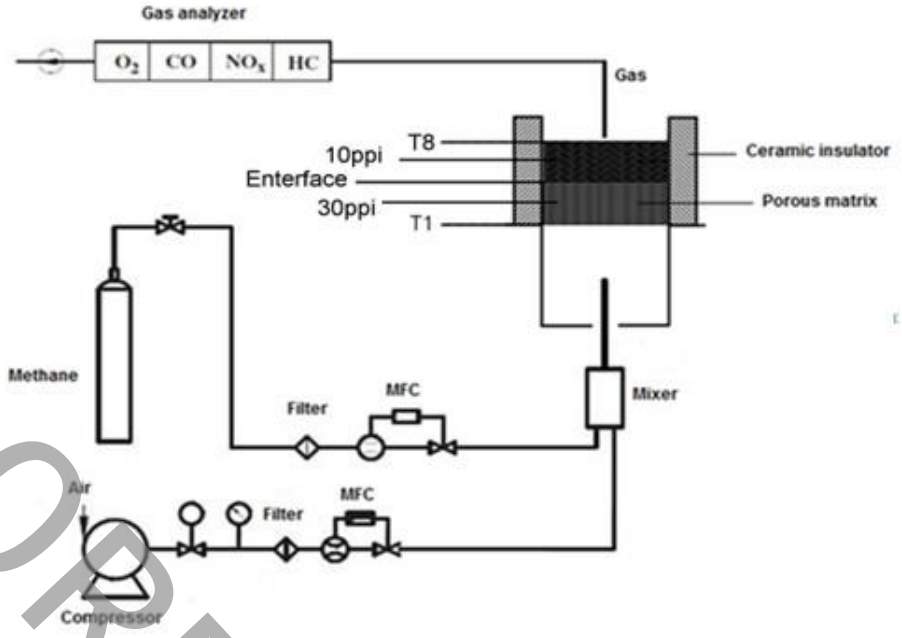

Fig. 1. Schematic view of the laboratory system

Table 1. Key properties of SiC, Al2O3 and ZrO2 [13]

Properties	Unit	SiC
Maximum air temperature	˚C	1600
The coefficient of thermal expansion α (20-100 ˚C)	10^{16} /K	4-5
Thermal Conductivity (λ) at 20˚C	W/m.K	80-150
Thermal Conductivity (λ) at 1000 ˚C	W/m.K	20-50
Specific heat capacity	J/g.K	0.7-0.8
Thermal stress resistance parameter, hard shock $R\left(\frac{\sigma}{E\alpha}\right)$	K	230
Thermal stress resistance parameter, medium thermal shock $R'(R\lambda)$	10^{-3} W/m	23
Total emissivity at 2000 K	-	0.9

Fig. 2. The position of the thermocouples on the retainer

Fig. 3. A submerged flame inside SiC foam

located exactly at the end of the second layer. A unit collects the thermocouples recordings versus time, and transfers them to a personal computer. Data is used then in a spreadsheet program for further processing. Two rotameters were used to measure the gas and air flow rates. The gas rotameter has a flow range of 0.1 to 10 Lit/min and an operating pressure of 16 mbarg under normal temperature conditions. Meanwhile, the working range of the air rotameter is 0.7-7 m^3/hr and its operating pressure is 50 mbarg.

3- Experimental Procedures and Results

3- 1- Experimental procedures

The experiments mainly conducted to determine the conditions in which a stable submerged flame is formed. The tests were carried out first by opening the gas valve to a certain point (considering the selected firing rate). Then, the flame was ignited by sparking over the burner surface. Under such circumstances, gas is burned with the surrounding air and a rich yellow free flame is formed above the burner. As the air valve is gradually opened, the equivalence ratio is reduced and the flame slowly turns blue beginning from its upstream zone and becomes shorter at the same time. Further increasing the air flow rate (reducing the equivalence ratio), the flame approaches the top of the ceramic porous medium, increasing the surface temperature of the medium which leads to turn the surface color to be slightly red. The condition corresponds to the surface flame regime taking place in rich mixtures. When the flame is attached to the surface, the air flow is kept constant, after a while the flame goes to the interface of the ceramic. The air flow rate is adjusted according to the equivalence ratio to be tested. Firing rate and equivalence ratio were both fixed from the early stage. The flame continues until completely stable and the flame regime at the firing rate is specified. The temperature measured by every thermocouple is logged from the moment the burner is started until the result is obtained. The apparatus cooled down after each test before the next one.

3- 2- Different flame regimes

After the flame penetration into the ceramic porous burner at a specified gas flow rate (a fixed FR), the air flow rate is adjusted to retain the specified equivalence ratio. In this situation, the flame may located at one of the following zones: on the top of the burner, below the first layer, and inside the porous medium (near the interface of the ceramic foams) as a submerged flame. Three situations may take place in that last case (submerged flame):

The flame gradually moves downstream and finally reach to the burner surface. This is known as blow-off.

After a while, the flame moves upstream until it reaches the zones below the first layer and completely exits the porous medium. This is known as flashback.

The flame remains near the interface for a long time. This condition is known as a stable submerged flame. This is the case that studied in the present work.

The firing rate of the burner is expressed as follows:

$$FR = \frac{LHV \times \dot{V}_f}{A} \quad (1)$$

where LHV is the low heat value of natural gas in terms of kJ/m^3, $\dot{V}_f$ is the flow rate of the gas in terms of m^3/s and A is the cross-section area of the burner in m^2.

3- 2- 1- Stable submerged flame regime

A flame is said to be stable so that the location of the flame remains unchanged for a minimum of 15 minutes (stability index time) near the interface. In most studies on similar porous media, the index time was assumed less than 15 minutes (e.g. Capatan [17] considered 10 minutes as the stability index time). During this period, the temperature at downstream and upstream of the flow might be slightly affected by the heat transfer between the ceramic pieces and the retainer, but the stability of the flame which is inferred by the axial temperature profile of the burner remains unchanged. Although the temperature at any point may change with time for many reasons, including the absence of a cooling mechanism in the retainer, but the maximum axial temperature at any time is associated with the thermocouple

Table 2. The position of the thermocouples on the retainer

Firing rate (kW/m^2)	Gas flow (lit/min)	Air flow (m^3/hr)	equivalence ratio	Mixture velocity (cm/s)
494	5	3.5	0.96	16.6
		4	0.84	18.77
		6	0.56	23.1
		7.5	0.45	34
		8.5	0.39	38.8
593	6	4	1	19
		4.8	0.84	22.5
		5	0.8	23.4
		7	0.57	32.15
		7.2	0.56	33
		8.1	0.5	36.9
		9	0.45	40.9
692	7	5.6	0.84	26.3
		8.4	0.56	38.5
		9.45	0.45	43.1

located near the interface of the layers. This indicates that the flame location is near the interface.

Fig. 3 shows a submerged flame, revealing that the burner surface radiates intensely. The conditions under which a submerged flame was formed are presented in Table 2. Considering Table 2, it is found that stability flame range is reduced by increasing the firing rate. In the submerged flame regime, thermocouples temperature increase at higher firing rate at a fixed equivalence ratio. Figs. 4 to 8 provide the axial temperature profiles of the burner in the case of submerged flames at different conditions. For most cases, the maximum temperature takes place near the interface of the two layers, showing that the flame is at this location. As is shown in figures, flame location has not changed in 15 minutes. The purpose of these diagrams is to indicate the location of the flame.

Fig. 4 illustrates the temperature against the axis of the layers at FR=494 kW/m^2 and φ=0.56. As shown in the figure, the maximum temperature takes place near the interface. All of the thermocouples measure the temperature of the side wall of the porous medium. Temperature distribution is plotted against the length of the burner in Fig. 5 at FR=593 kW/m^2 and φ=0.56 (the same as that of the previous case). The flame is formed at the same point, but the temperature gradient increases before the formation of the flame. This can be attributed to higher flow rate of the air-gas mixture.

The temperature distribution is plotted in Fig. 6 at FR=494 kW/m^2 (the same as that of the first case) and φ=0.84. This figure was plotted for comparison with Fig. 4 and to investigate the effect of equivalence ratio at a fixed firing rate. Comparing Figs. 4 and 6, it is concluded that increasing the equivalence ratio leads to a higher maximum temperature. This was anticipated since the flame temperature increases due to increasing equivalence ratio.

Figs. 7 and 8 show an example of flashback and blow-off. As shown in Fig. 7, the flame is first formed near the interface and then the flame moves to the upstream over time. Eventually at t=400 s flashback occurs and the flame completely exits the porous medium. Fig. 8 show an example of blow-off. At first, the flame is formed near the interface and finally at t=180 s flame moves to downstream and ultimately blow-off occurs.

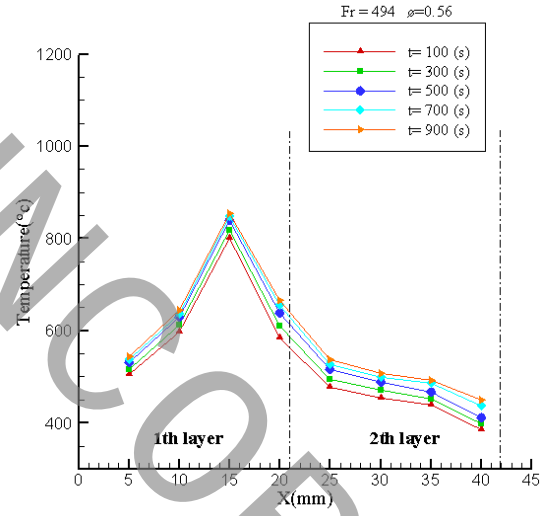

Fig. 4. Axial temperature gradient of the burner for testing at φ=0.56, and FR=494 kW/m2

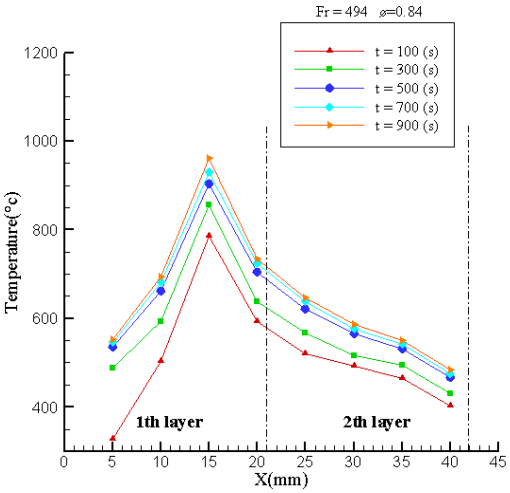

Fig. 6. Axial temperature gradient of the burner for testing at φ=0.84, and FR=494 kW/m2

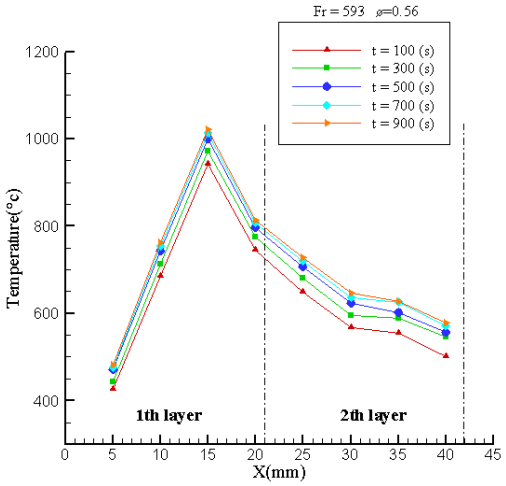

Fig. 5. Axial temperature gradient of the burner for testing at φ=0.56, and FR=593 kW/m2

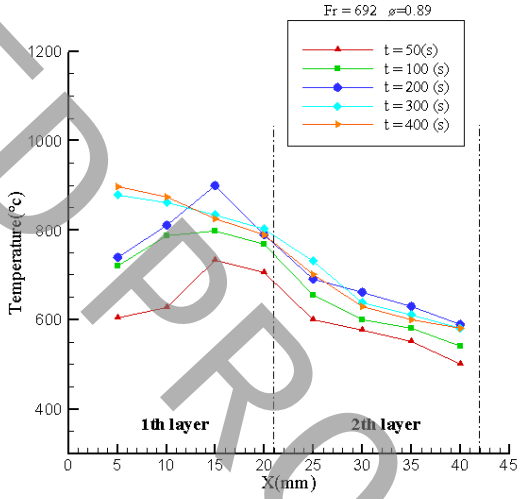

Fig. 7. Axial temperature gradient of the burner for testing at φ=0.89 and FR=692 kW/m2

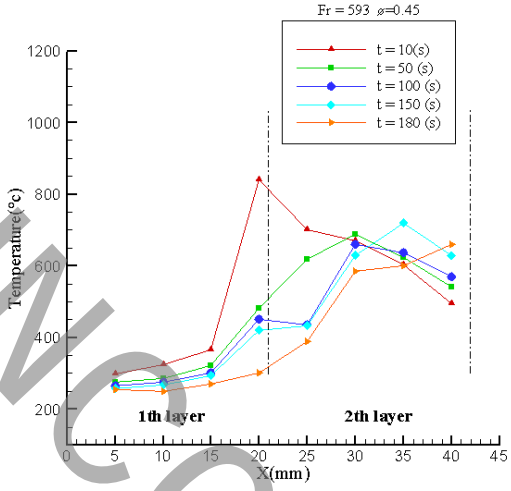

Fig. 8. Axial temperature gradient of the burner for testing at φ=0.45, and FR=593 kW/m2

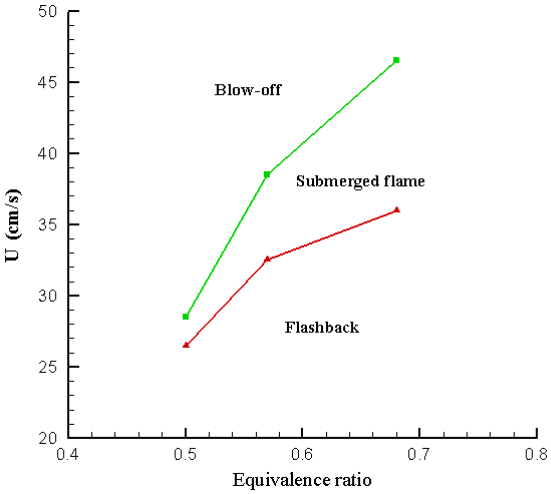

Fig. 10. Flame stability characteristic diagrams at various equivalence ratios

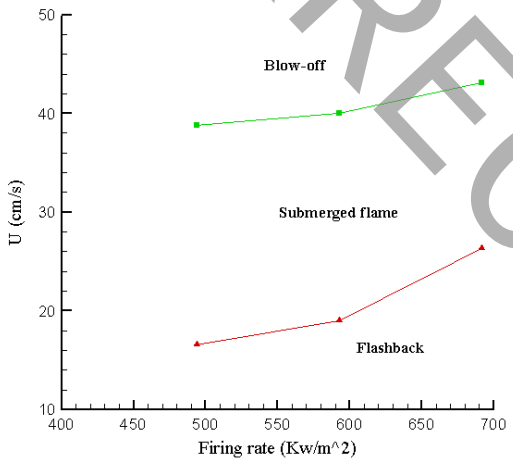

Fig. 9. Flame stability characteristic diagrams at various firing rates

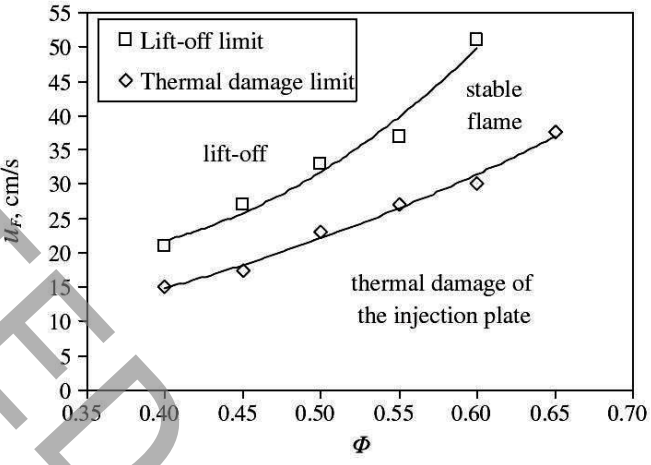

Fig. 11. Flame stability characteristic diagrams for the burner studied by Capatan et al. [17]

In order to demonstrate the combustion regimes that took place in the experiments, the corresponding equivalence ratio, firing rate and mixture velocity ranges for blow-off, flashback, and submerged flame are presented in Figs. 9 and 10. The behavior is similar to what was reported by Capatan et al. [17] as depicted in Fig. 11. According to Fig. 9, by increasing the firing rate, stability range decreases. As shown in the Fig. 10, by increasing the equivalence ratio, velocity range increases. Another interesting point in Figs. 9 and 10 is that the combustion regime is changed to flashback regime by increasing the equivalence ratio at a fixed mixture velocity. Increasing the input flow rate results in a situation where convection heat transfer (from solid to gas network) becomes greater than heat generation. Therefore, flow velocity becomes larger than the flame velocity, and the flame gradually leaves the burner at its downstream and eventually blows off.

4- Error Analysis

All experiments were conducted three times to make sure consistency and repeatability of the results. The measured data were almost the same which proves repeatability and accuracy of the results. According to the specification of the measurement instrument, the accuracy of the gas and air flow rates are 2% of the full scale. Uncertainty of the dependent parameter of R is determined as [18]:

$$W_R = \left[\left(w_1 \frac{\partial R}{\partial x_1} \right)^2 + \left(w_2 \frac{\partial R}{\partial x_2} \right)^2 + \ldots + \left(w_n \frac{\partial R}{\partial x_n} \right)^2 \right]^{\frac{1}{2}} \quad (2)$$

Table 3. The amount of uncertainty of the firing rate and the equivalence ratio

Firing rate (kW/m^2)	equivalence ratio	Uncertainty of the equivalence ratio %	Uncertainty of the firing rate %
494	0.96	5.4	3.6
	0.84	4.4	
	0.56	2.6	
	0.45	2	
	0.39	1.7	
593	1	4.5	3.2
	0.84	3.7	
	0.8	3.5	
	0.57	2.13	
	0.56	2.1	
	0.5	1.9	
	0.45	1.6	
692	0.84	3.2	2.8
	0.56	1.8	
	0.45	1.4	

where W_R is the uncertainty of the dependent parameter of R and w_1, …, w_n are the uncertainty of the independent parameters of x_1,…, x_n. In this study, equivalence ratio and firing rate are two dependent parameters. The calculated uncertainty of the equivalence ratio and firing rate are presented in Table 3.

5- Conclusions

In this paper, an experimental study is presented for the combustion of natural gas-air mixtures in a two-layer porous burner (the first layer is 30 ppi and the second layer is 10 ppi). The condition in which a submerged flame is formed have been evaluated for three firing rate at various equivalence ratios. The results are compared with another experimental results which shows a good consistency between them. In both of them the stability limit extends with increasing lean equivalence ratio. An example of blow-off and flashback has been shown. The conclusion of this work can be summarized as follows.

Flame stability limit is reduced by increasing the firing rate.

The location of the flame greatly depends on the equivalence ratio.

Combustion at a fixed equivalence ratio becomes more unstable as the input mix flow rate is increased.

In the submerged flame regime, a higher firing rate at fixed equivalence ratio leads to higher temperatures.

Reducing the equivalence ratio extends flashback time.

The maximum temperature takes place near the interface of the two layers.

Nomenclature

A	Cross-section area (m^2)
FR	Firing Rate (kW/m^2)
LHV	Low heat value (kJ/m^3)
U	Mixture velocity
$\dot{V}_f$	Flow rate (m^3/s)
W	Uncertainty
ppi	Pores per inch
φ	Equivalence ratio

References

[1] W. FJ, Combustion temperature - the future, Nature, 233 (1971) 239–241.

[2] L. Younis, R. Viskanta, Experimental determination of the volumetric heat transfer coefficient between stream of air and ceramic foam, International journal of heat and mass transfer, 36(6) (1993) 1425-1434.

[3] V. Khanna, R. Goel, J. Ellzey, Measurements of emissions and radiation for methane combustion within a porous medium burner, Combustion science and technology, 99(1-3) (1994) 133-142.

[4] J. Randrianalisoa, Y. Bréchet, D. Baillis, Materials selection for optimal design of a porous radiant burner for environmentally driven requirements, Advanced Engineering Materials, 11(12) (2009) 1049-1056.

[5] A. Bakry, A. Al-Salaymeh, H. Ala'a, A. Abu-Jrai, D. Trimis, Adiabatic premixed combustion in a gaseous fuel porous inert media under high pressure and temperature: Novel flame stabilization technique, Fuel, 90(2) (2011) 647-658.

[6] C. Keramiotis, B. Stelzner, D. Trimis, M. Founti, Porous burners for low emission combustion: An experimental investigation, Energy, 45(1) (2012) 213-219.

[7] J.-R. Shi, C.-M. Yu, B.-W. Li, Y.-F. Xia, Z.-J. Xue, Experimental and numerical studies on the flame instabilities in porous media, Fuel, 106 (2013) 674-681.

[8] H. Wang, C. Wei, P. Zhao, T. Ye, Experimental study on temperature variation in a porous inert media burner for premixed methane air combustion, Energy, 72 (2014) 195-200.

[9] H. Gao, Z. Qu, X. Feng, W. Tao, Combustion of methane/air mixtures in a two-layer porous burner: A comparison of alumina foams, beads, and honeycombs, Experimental Thermal and Fluid Science, 52 (2014) 215-220.

[10] B. Stelzner, C. Keramiotis, S. Voss, M. Founti, D. Trimis, Analysis of the flame structure for lean methane–air combustion in porous inert media by resolving the hydroxyl radical, Proceedings of the Combustion Institute, 35(3) (2015) 3381-3388.

[11] S.A. Shakiba, R. Ebrahimi, M. Shams, Z. Yazdanfar, Effects of foam structure and material on the performance of premixed porous ceramic burner, Proceedings of the Institution of Mechanical Engineers, Part A: Journal of Power and Energy, 229(2) (2015) 176-191.

[12] Y. Liu, A. Fan, H. Yao, W. Liu, A numerical investigation on the effect of wall thermal conductivity on flame stability and combustion efficiency in a mesoscale channel filled with fibrous porous medium, Applied Thermal Engineering, 101 (2016) 239-246.

[13] M.D. Emami, H. Atoof, M. Rezaeibakhsh, Flash-Back Phenomenon in a Two-Layer Porous Media: An Experimental Study, Journal of Porous Media, 19(3) (2016).

[14] S.A. Ghorashi, S.A. Hashemi, S.M. Hashemi, M. Mollamahdi, Experimental study on pollutant emissions in the novel combined porous-free flame burner, J Energy, 162 (2018) 517-525.

[15] S.M. Hashemi, S.A. Hashemi, Flame stability analysis of the premixed methane-air combustion in a two-layer porous media burner by numerical simulation, J Fuel, 202 (2017) 56-65.

[16] S.M. Hashemi, S.A. Hashemi, Numerical study of the flame stability of premixed methane–air combustion in a combined porous-free flame burner, J Proceedings of the Institution of Mechanical Engineers, Part A: Journal of PowerEnergy, (2018) 0957650918790662.

[17] R. Catapan, A. Oliveira, M. Costa, Non-uniform velocity profile mechanism for flame stabilization in a porous radiant burner, Experimental Thermal and Fluid Science, 35(1) (2011) 172-179.

[18] J.P. Holman, W.J. Gajda, Experimental methods for engineers, McGraw-Hill New York, 2001.